TDA Progress Report 42-99

November 15, 1989



# Photon Statistical Limitations for Daytime Optical Tracking

W. M. Folkner and M. H. Finger
Tracking Systems and Applications Section

*Tracking of interplanetary spacecraft equipped with optical communications systems by using astrometric instruments is being investigated by JPL. Existing instruments are designed to work at night and, for bright sources, are limited by tropospheric errors. To provide full coverage of the solar system, astrometric tracking instruments must either be capable of daytime operation or be space-based. The integration times necessary for the ground-based daytime photon statistical errors to reach a given accuracy level (5 to 50 nanoradians) have been computed for an ideal astrometric instrument. The required photon statistical integration times are found to be shorter than the tropospheric integration times for the ideal detector. Since the astrometric accuracy need not be limited by photon statistics even under daytime conditions, it may be fruitful to investigate instruments for daytime optical tracking.*

## I. Introduction

Several observables for spacecraft navigation based on a laser telemetry system are being investigated. One such observable is the difference in direction between the spacecraft and a cataloged reference object in the same field of view of an astrometric telescope. The error for such a ground-based differential astrometric measurement includes the directional error of the reference source, the photon statistical error, and the error induced by index of refraction fluctuations in the troposphere. The best conditions for making differential astrometric measurements are at night, when the low background light levels lead to small statistical errors, and at high angles of elevation above the horizon, where the troposphere errors are smallest due to the short path length through the atmosphere.

Unfortunately, on any given day only a small portion of the solar system can be observed at high elevations during the night. In Section II, the daily available observation times for the planets are examined for the cases in which observations are restricted to nighttime and limited in elevation. All the planets suffer seasons in which no nighttime viewing is possible, corresponding to periods of low Sun-Earth-Probe (SEP) angles. While nighttime angular position measurements might augment other observable types during a fraction of a mission, critical parts of

a mission may take place at low SEP angles due to launch criteria. The restricted nighttime visibility implies that ground-based astrometric observations of laser-equipped spacecraft may have to cope with the daytime sky background.

In Section III, the photon statistical error of an astrometric measurement in the presence of a background is analyzed. In Section IV, some specific examples of the photon statistical error are presented. In Section V, a simple model of the tropospheric error is discussed. The relative size of these errors is affected by the angular separation of the reference source and the spacecraft. A larger separation is more likely to allow the use of brighter reference objects and result in a smaller photon statistical error. A small separation would require the utilization of fainter reference objects but would decrease the tropospheric error. The smallest usable field of view is set by the density of the catalog stars. It was expected that in the mid 1990s the Hipparchos mission would provide a catalog with an average of 2.5 stars per 1-degree by 1-degree field with initial accuracy of 10 nrad per component and proper motion uncertainty of 10 nrad/year [1]. The average brightness of reference sources in a 1-degree by 1-degree field is magnitude $m_v = 8$ [2]. Using magnitude $m_v = 8$ and 1 degree for the source-spacecraft separation, it is found that the integration times for daytime observations with 50 nrad accuracy are about 30 minutes.

For the error models used here, the tropospheric error for such measurements is larger than the photon statistical error. However, the daytime photon signal-to-noise ratio is very unfavorable. Existing astrometric instruments, designed for nighttime operation, are not able to work in this regime. Limitations imposed by real detectors or by systematic effects such as sky brightness variation may be much larger than the photon statistical error.

## II. Nighttime Planetary Viewing Limitations

To demonstrate what fraction of a mission trajectory would be inaccessible to nighttime astrometric measurements, the number of minutes per day that each planet is visible from Goldstone in the night sky has been computed. Here "night" has been defined as the time that the sun is below $-15$ degrees elevation. This value for sun elevation was chosen to correspond roughly to the time of astronomical darkness. Since the astrometric error depends on elevation angle through the elevation dependence of the troposphere, two different minimum elevation cutoffs for the planets were included.

Figures 1–7 are plots of the number of minutes per day that Venus, Mars, Jupiter, and Saturn are above 10 degrees or 30 degrees elevation with the sun below $-15$ degrees for the time span of 1990 to 2000. Mercury is almost never visible in the dark sky and is not plotted. Venus is always at low elevation, and nighttime astrometric tracking is possible less than half of each year. The outer planets are unavailable for 25 percent or more of each year. These figures suggest that visibility limitations will severely affect the utility of astrometric tracking if it is limited to the nighttime hours.

## III. Photon Statistics of an Astrometric Telescope

This section presents an estimate of the accuracy limitation placed by photon statistics on an astrometric telescope in the daytime. This category includes Ronchi-ruled telescopes and charge-coupled device (CCD) instruments. An ideal detector is able to record the position on the focal plane for each detected photon. Any real instrument will have larger photon statistical errors than this ideal instrument. CCD instruments are capable of dividing the image of a point source into many pixels and can approach the ideal detector scheme. However, limits on the size of CCD arrays limit the fields of view of such instruments. In a Ronchi telescope, a moving ruling is used to modulate the light incident on the detector with position information derived from the detected modulation [3]. For present designs, the field of view must be larger than the image of the star. This makes Ronchi telescopes more susceptible to background light problems than CCD instruments.

The ideal astrometric telescope tracks a source for a time $T$ and records the plane-of-sky coordinates $(\xi, \eta) = \vec{\Omega}$ for each photon detected. The troposphere and instrument resolution cause the photons to be smeared in the plane of the sky. For simplicity, the photon spatial distribution about the true source direction is assumed to have the Gaussian form

$$I(\vec{\Omega} - \vec{\Omega}_s) = BT + \frac{ST}{2\pi\sigma^2} \exp\left[-\frac{(\vec{\Omega} - \vec{\Omega}_s)^2}{2\sigma^2}\right] \quad (1)$$

where $B$ is the number of background photons per unit solid angle per unit time, $\vec{\Omega}_s$ is the true source direction, and $S$ is the number of signal photons per unit time. This distribution is a reasonable approximation to a smeared point source in a uniform background and has been successfully used in fitting high-precision small-field images [4]. The width of the Gaussian is determined by the ap-

parent diameter of a point source. This apparent diameter as determined by the turbulence of the atmosphere is commonly called the seeing angle. The full width at half maximum of the Gaussian ($2.35\sigma$) is here set equal to the seeing angle.

Measurement of the source direction consists of recording the arrival of $n$ photons and the plane-of-sky coordinates for each detected photon. The maximum-likelihood method can be used to estimate the source direction. The likelihood function $L(\vec{\Omega}_a)$ is the probability of recording $n$ photons with the set of arrival directions $\{\vec{\Omega}_k\}$ given an assumed source direction $\vec{\Omega}_a$.

The photons are distributed in time according to Poisson statistics. The expected number of detected photons is given by

$$N = \int I(\vec{\Omega}) d^2\Omega \tag{2}$$

where the integral is taken over the field of view of the telescope. The probability of detecting $n$ photons is then given in [5] as

$$P(n) = \frac{N^n e^{-N}}{n!} \tag{3}$$

The (normalized) probability of any one photon arriving with direction $\vec{\Omega}_k$ given that the source is at direction $\vec{\Omega}_a$ is

$$P(\vec{\Omega}_k|\vec{\Omega}_a) = \frac{I(\vec{\Omega}_k - \vec{\Omega}_a)}{N} \tag{4}$$

Assuming that the distribution for each photon-arrival direction is independent, the probability of finding $n$ photons with the set of photon directions $\{\vec{\Omega}_k\}$ is

$$L(\vec{\Omega}_a) = \left(\frac{N^n e^{-N}}{n!}\right) \prod_{k=1}^{n} \frac{I(\vec{\Omega}_k - \vec{\Omega}_a)}{N} \tag{5}$$

The maximum-likelihood estimate of the source direction is the assumed source direction that maximizes the likelihood function. In the limit $N \gg 1$ the error associated with this estimate is given by the Konig-Kramer bound [6]

$$\frac{1}{\sigma_\xi^2} = \left\langle -\frac{\partial^2 \log L(\vec{\Omega}_a)}{\partial \xi_a^2} \right\rangle \Bigg|_{\vec{\Omega}_s} \tag{6}$$

where $\sigma_\xi^2$ is the variance of the source direction estimate in the $\xi$ direction, and the expectation value is the average taken over all possible numbers of detected photons and sets of directions. Since the assumed photon distribution is symmetric, the error is the same for the $\eta$ direction. With some work, the error expression of Eq. (6) can be applied to the likelihood function given in Eq. (5) to give the error in the source direction measurement as

$$\sigma_\xi^2 = \frac{\sigma^2}{ST} f\left(\frac{2\pi\sigma^2 B}{S}\right) \tag{7}$$

where the function $f(\alpha)$ is given by

$$f(\alpha) = \left[\frac{1}{2}\int_0^\infty \frac{x^3 e^{-x^2}}{\alpha + e^{-x^2/2}}\, dx\right]^{-1} \tag{8}$$

In the limit of no background ($B = 0$), $\alpha = 0$, and $f(0) = 1$; the directional error is then given by

$$\sigma_\xi = \frac{\sigma}{\sqrt{ST}} \tag{9}$$

Rewriting Eq. (9) gives the integration time to reach a specified accuracy $\sigma_\xi$ as

$$T = \frac{\sigma^2}{\sigma_\xi^2 S} \tag{10}$$

In the limit of high background, the position error is given by

$$\sigma_\xi = \frac{\sigma}{\sqrt{ST}} \sqrt{\frac{8\pi\sigma^2 B}{S}} \tag{11}$$

Rewriting Eq. (11) gives

$$T = \left(\frac{\sigma^2}{\sigma_\xi^2 S}\right)\left(\frac{8\pi\sigma^2 B}{S}\right) \tag{12}$$

The effective signal-to-noise ratio for determining the source direction is $S/(8\pi\sigma^2 B)$ where the combination $8\pi\sigma^2 B$ is the effective background rate.

## IV. Examples of Photon Statistical Integration Times

In this section, the integration times needed to reach a given accuracy for a reference star and for a spacecraft at 10 AU with a 2-W laser are given. The parameters assumed for the detector, the spacecraft, and the background

are summarized in Table 1. The derived photon rates and integration times are listed in Table 2.

The photon rate from a star of visual magnitude $m_v$ is given by [2, 7] as approximately

$$S = 10^{-0.4m_v - 7.45} \frac{\mathrm{W}}{\mu\mathrm{m}\, m^2} \left(\frac{\lambda}{hc}\right) \Delta\lambda \frac{\pi}{4} d_r^2 \eta_a \eta_{ra} \eta_{ro} \eta_f \eta_d \tag{13}$$

where $\lambda$ is the central wavelength, $h$ is Planck's constant, $c$ is the speed of light, $\Delta\lambda$ is the wavelength pass band, $d_r$ is the telescope diameter, $\eta_a$ is the atmosphere transmission factor, $\eta_{ra}$ is the receiver obscuration factor, $\eta_{ro}$ is the receiver optics efficiency, $\eta_f$ is the narrow-band filter efficiency, and $\eta_d$ is the detector quantum efficiency. Since refraction will cause image smearing if the wave band is too wide, a value $\Delta\lambda = 0.1$ $\mu$m, centered at $\lambda = 0.532$ $\mu$m, will be used below. For the receiver efficiencies given in Table 1 and for a star of magnitude $m_v = 8$ the signal rate is $6.8 \times 10^5$ photons/second.

The photon rate received from the spacecraft is given by [7] as

$$S = P_l \left(\frac{\lambda}{hc}\right) \left(\frac{\pi d_t}{\lambda}\right)^2 \left(\frac{\lambda}{4\pi r}\right)^2 \left(\frac{\pi d_r}{\lambda}\right)^2 \times \eta_{ta} \eta_{to} \eta_{tp} \eta_a \eta_{ra} \eta_{ro} \tag{14}$$

where $P_l$ is the transmitted laser power, $\lambda$ is the wavelength, $d_t$ is the transmitter objective diameter, $r$ is the spacecraft-receiver distance, $\eta_{ta}$ is the transmitter obscuration factor, $\eta_{to}$ is the transmitter optics efficiency, and $\eta_{tp}$ is the transmitter pointing efficiency. The parameters used here are taken from an example by Kerr [8] and listed in Table 1. These factors combined with the nominal receiver used above yield a detected photon rate $S$ of $2.6 \times 10^4$ photons/second for the spacecraft.

A critical parameter for the tracking telescope is the atmospheric seeing. At many sites, the daytime seeing is worse than the nighttime seeing by a factor of 5 to 10 [9, 10]. However, at some solar observatory sites, the seeing is 5 to 10 $\mu$rad ($\sim$1 to 2 arcseconds) both day and night. At the Sacramento Peak site, the daytime seeing angle is reported as being less than 10 $\mu$rad 80 percent of the time and better than 5 $\mu$rad 50 percent of the time during the day [11]. Since 10 $\mu$rad is similar to other reported daytime seeing values (see [11] and references therein), 10 $\mu$rad full width at half maximum will be taken as a nominal value. This corresponds to a value $\sigma = 4.3$ $\mu$rad for the photon distribution.

The background photon rate is given by

$$(8\pi\sigma^2)B = (8\pi\sigma^2)\, I \left(\frac{\lambda}{hc}\right) \Delta\lambda \frac{\pi}{4} d_r^2 \eta_{ro} \eta_{ra} \eta_f \eta_d \tag{15}$$

where $I$ is the background spectral irradiance. The daytime background spectral irradiance depends on the weather, the sun elevation, and the Sun-Earth-Probe angle among other factors. The value for $I$ of 100 W/($\mu$m $m^2$ steradian) at 0.532 $\mu$m [12] will be used in the following example. Kerr gives values ranging from 30 W/($\mu$m $m^2$steradian) at 90 degrees from the sun to 500 W/$\mu$m $m^2$ steradian at 10 degrees to the sun [8]. Using the receiver values of Table 1 and 2-arcsec seeing, the daytime background rate is $2.6 \times 10^9$ photons/second. Using a narrower filter will not improve the signal-to-noise ratio for the reference star since the signal photon rate depends on the bandwidth in the same way as the background; narrowing the filter bandwidth reduces the signal rate and increases the needed integration time. However, the laser signal is narrow band and narrowing the filter bandwidth improves the spacecraft signal-to-noise ratio.

Table 2 presents the integration times needed to reach 50-nrad or 5-nrad accuracy for the reference star and the spacecraft. Several different filter bandwidth options have been used. For the case of the 0.03-nm filter, the filter transmission efficiency is reduced to 0.4 [8]. The integration times for the photon statistics error to reach the 5-nrad level are not prohibitively long provided that the spacecraft and star are separately filtered. However, several factors may combine to lengthen the integration times. The photon rates for the reference star plus background are very high for photon counting devices. Detector dead time and noise will be significant effects. A Ronchi telescope integrates the background over a fixed field of view. Unless the field of view is limited to the size of the source image and precisely positioned, the photon statistics error will be much worse for a Ronchi telescope. In any case, the ruling modulation reduces the photon flux by a factor of 2, correspondingly increasing the integration time. If each coordinate is measured separately, the times will double again.

Effects other than counting problems are important. Since the integration time increases as the fourth power of the seeing, the site selection is critical. For the reference star, the signal-to-noise ratio may be worse than $10^{-3}$. This may pose unrealistic requirements on the dynamic range and linearity of the detector. There is also the possibility that variations in the background intensity

over the period of integration could degrade the accuracy of the star position.

## V. Tropospheric Integration Times

The photon statistics contribute an angular position error for the spacecraft and the reference object. The error in the angular difference between the spacecraft and reference object is also affected by variations in angle of arrival imposed by the troposphere. The integration time requirements imposed by the troposphere may be computed from a result by Lindegren [13]. Lindegren's result is derived from a frozen turbulence model of the atmosphere with a power law structure function. The turbulence causes angle of arrival variation as the frozen turbulence moves with the wind velocity. The variations in angle of arrival from two point sources are computed, given some assumptions about the atmosphere structure and averaging over wind direction. Lindegren's paper compares his model to several experimental results, including stellar position and solar diameter measurements, with reasonable agreement.

The expression for the error $\sigma_\theta$ in the difference angle $\theta$ between two sources is

$$\sigma_\theta = 6.3 \times 10^{-6} \theta^{\frac{1}{2}} T^{-\frac{1}{2}} \tag{16}$$

where $\sigma_\theta$ and $\theta$ are given in radians and the integration time $T$ in seconds. Solving Eq. (16) for the integration time necessary for a given angular accuracy $\sigma_\theta$ gives

$$T = 4.0 \times 10^{-11} \theta^{\frac{1}{2}} \sigma_\theta^{-2} \tag{17}$$

This expression applies near zenith and with about 1-arcsec seeing. Results are expected to be worse for lower elevation angles and worse seeing.

For two objects 1 degree apart, this implies an integration time of 59 hours to reach 5-nrad accuracy and 35 minutes to reach 50-nrad accuracy. These times are long compared to those imposed by the photon statistics for a magnitude 8 star. There is a possible trade-off by narrowing the field of view and utilizing fainter reference stars. However, this implies a larger catalog effort. By including more reference objects in the field, there is the possibility of reducing the troposphere error.

## VI. Discussion

The photon statistics do not rule out the operation of astrometric telescopes for daytime optical tracking of spacecraft. Given the simple assumptions used in Section III, the tropospheric error dominates the photon statistical error for a magnitude $m_v = 8$ star and 1-degree source-spacecraft separation. However, existing instruments are not capable of operating in the daytime because of the extremely poor signal-to-noise ratio and large photon fluxes. Finding a suitable detection scheme for daytime operation will be a challenge. Since the integration times required are many minutes, systematic effects and variations in the background level may wash out the position signal. It would be useful to try differential position measurement in the daytime at a solar observatory with a CCD camera to begin an investigation into systematic background effects.

## References


[1] J. Kovalevsky, "Prospects for Space Stellar Astrometry," *Space Science Review*, vol. 39, pp. 1–63, 1984.

[2] B. L. Schumaker, "Apparent Brightness of Stars and Lasers," *TDA Progress Report 42-93*, vol. January–March 1988, Jet Propulsion Laboratory, Pasadena, California, pp. 111–130, May 15, 1988.

[3] G. D. Gatewood, "The Multichannel Astrometric Photometer and Atmospheric Limitations in the Measurement of Relative Positions," *Astron. J.*, vol. 94, pp. 213–224, 1987.

[4] D. G. Dahn and C. C. Monet, "CCD Astrometry. I. Preliminary Results from the KPNO 4-m/CCD Parallax Program," *Astron. J.*, vol. 88, pp. 1489–1507, 1983.

[5] P. R. Bevington, *Data Reduction and Error Analysis for the Physical Sciences*, San Francisco: McGraw-Hill, 1969.

[6] M. Fisz, *Probability Theory and Mathematical Statistics*, New York: John Wiley and Sons, 1963.

[7] W. K. Marshall and B. D. Burk, "Received Optical Power Calculations Link Performance Analysis," *TDA Progress Report 42-87*, vol. July–September 1986, Jet Propulsion Laboratory, Pasadena, California, pp. 32–40, November 15, 1986.

[8] E. L. Kerr, "Fraunhofer Filters to Reduce Solar Background for Optical Communications," *TDA Progress Report 42-87*, vol. July–September 1986, Jet Propulsion Laboratory, Pasadena, California, pp. 48–55, November 15, 1986.

[9] E. S. Barker, "Site Testing with an Acoustic Sounder at McDonald Observatory," *Identification, Optimization, and Protection of Optical Telescope Sites*, R. L. Millis, O. G. Franz, H. D. Ables, and C. C. Dahn (eds.), Lowell Observatory, pp. 49–57, 1987.

[10] D. A. Erasmus, "Identification of Optimum Sites for Daytime and Nighttime Observations at Mauna Kea Observatory," *Identification, Optimization, and Protection of Optical Telescope Sites*, R. L. Millis, O. G. Franz, H. D. Ables, and C. C. Dahn (eds.), Lowell Observatory, pp. 86–93, 1987.

[11] P. N. Brandt, H. A. Mauter, and R. Smartt, "Day-time seeing statistics at Sacramento Peak Observatory," *Astron. Astrophys.*, vol. 188, pp. 163–168, 1987.

[12] W. K. Pratt, *Laser Communication Systems*, New York: John Wiley and Sons, 1969.

[13] L. Lindegren, "Atmospheric Limitations of Narrow-field Optical Astrometry," *Astron. Astrophys.*, vol. 89, pp. 41–47, 1980.

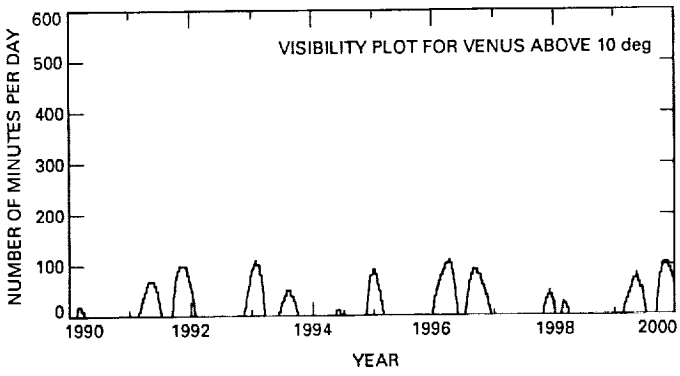


**Fig. 1. Plot of the number of minutes per day (24 hours) for which Venus is visible above 10 degrees in the nighttime sky.**

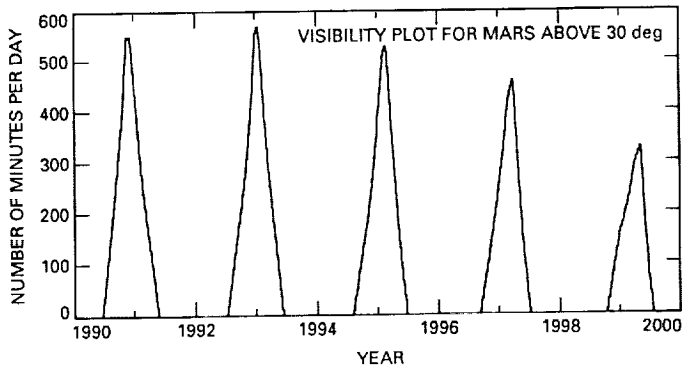


**Fig. 3. Plot of the number of minutes per day (24 hours) for which Mars is visible above 30 degrees in the nighttime sky.**

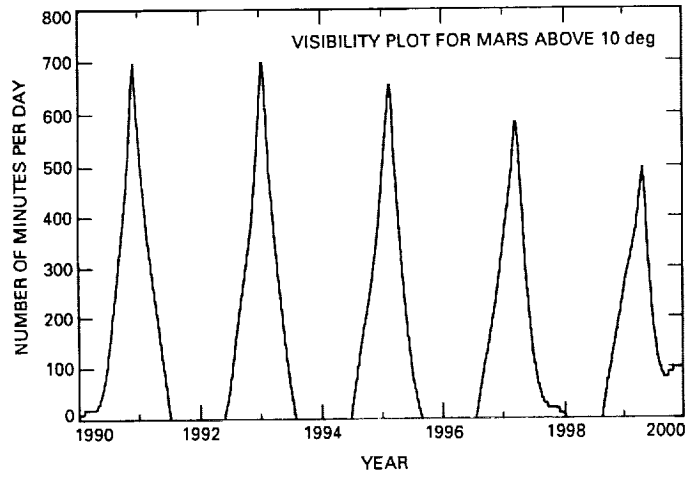


**Fig. 2. Plot of the number of minutes per day (24 hours) for which Mars is visible above 10 degrees in the nighttime sky.**

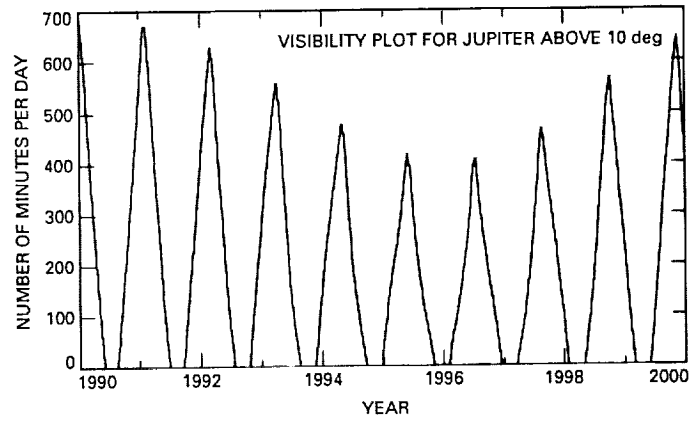


**Fig. 4. Plot of the number of minutes per day (24 hours) for which Jupiter is visible above 10 degrees in the nighttime sky.**

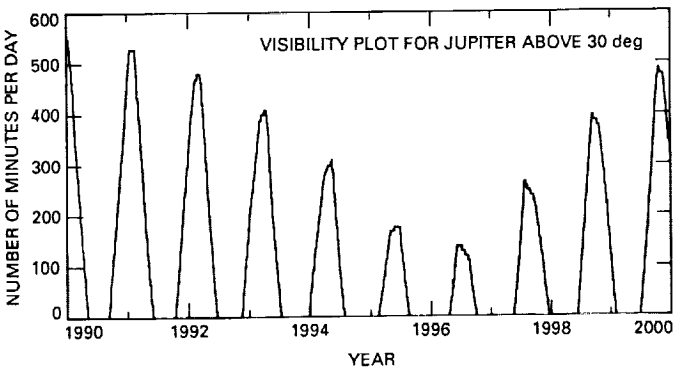


**Fig. 5. Plot of the number of minutes per day (24 hours) for which Jupiter is visible above 30 degrees in the nighttime sky.**

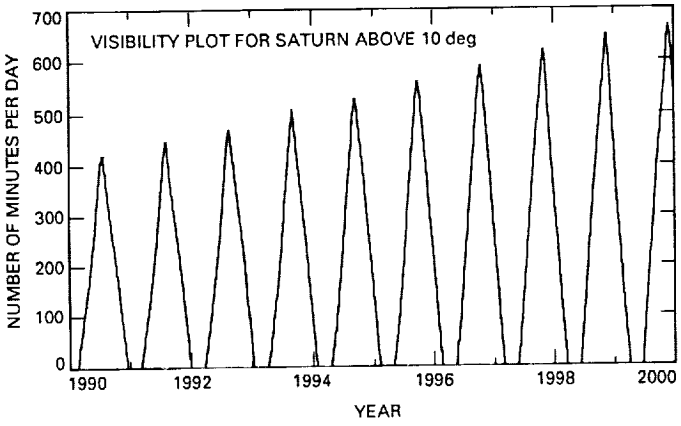


**Fig. 6. Plot of the number of minutes per day (24 hours) for which Saturn is visible above 10 degrees in the nighttime sky.**

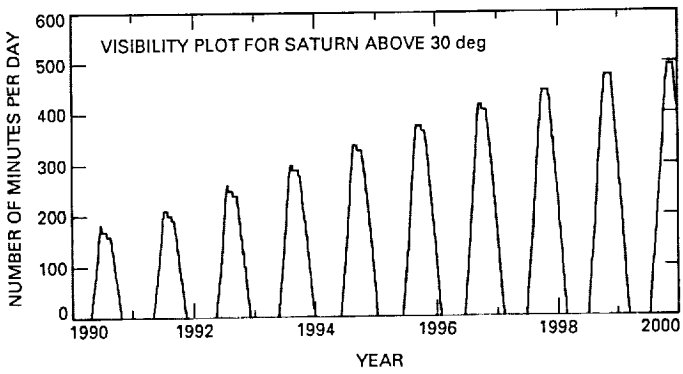


**Fig. 7. Plot of the number of minutes per day (24 hours) for which Saturn is visible above 30 degrees in the nighttime sky.**